

Assessing the Cone Photoreceptor Mosaic in Eyes with Pseudodrusen and Soft Drusen In Vivo Using Adaptive Optics Imaging

Sarah Mrejen, MD,^{1,2} Taku Sato, MD,^{1,2} Christine A. Curcio, PhD,³ Richard F. Spaide, MD,^{1,2}

Purpose: To investigate the cone photoreceptor mosaic in eyes with pseudodrusen as evidenced by the presence of subretinal drusenoid deposits (SDD) and conventional drusen using adaptive optics (AO) imaging integrated into a multimodal imaging approach.

Design: Observational case series.

Participants: Eleven patients (11 eyes) with pseudodrusen and 6 patients (11 eyes) with conventional drusen.

Methods: Consecutive patients were examined using near-infrared reflectance (IR) confocal scanning laser ophthalmoscopy (SLO) and eye-tracked spectral-domain optical coherence tomography (SD-OCT) and flood-illuminated retinal AO camera of nonconfluent pseudodrusen or conventional drusen. Correlations were made between the IR-SLO, SD-OCT, and AO images. Cone density analysis was performed on AO images within $50 \times 50\text{-}\mu\text{m}$ windows in 5 regions of interest overlying and in 5 located between SDD or conventional drusen with the same retinal eccentricity.

Main Outcome Measures: Cone densities in the regions of interest.

Results: The pseudodrusen correlated with subretinal accumulations of material in SD-OCT imaging and this was confirmed in the AO images. Defects in the overlying ellipsoid zone band as seen by SD-OCT were associated with SDD but not conventional drusen. The mean \pm standard deviation cone density was 8964 ± 2793 cones/mm² between the SDD and 863 ± 388 cones/mm² over the SDD, a 90.4% numerical reduction. By comparison the mean cone packing density was 9838 ± 3723 cones/mm² on conventional drusen and 12595 ± 3323 cones/mm² between them, a 21.9% numerical reduction. The difference in cone density reduction between the two lesion types was highly significant ($P < 0.001$).

Conclusions: The pseudodrusen in these eyes correlated with subretinal deposition of material in multiple imaging modalities. Reduced visibility of cones overlying SDD in the AO images can be because of several possible causes, including a change in their orientation, an alteration of their cellular architecture, or absence of the cones themselves. All of these explanations imply that decreased cone photoreceptor function is possible, suggesting that eyes with pseudodrusen appearance may experience decreased retinal function in age-related macular degeneration independent of choroidal neovascularization or retinal pigment epithelial atrophy.

Financial Disclosure(s): Proprietary or commercial disclosure may be found after the references. *Ophthalmology* 2013;■:1–7 © 2013 by the American Academy of Ophthalmology.

Age-related macular degeneration (AMD) is a progressive disorder and the leading cause of irreversible visual impairment in individuals >65 years in the developed world.^{1–3} Drusen are a hallmark of nonneovascular AMD. Two main clinical phenotypes—conventional drusen and pseudodrusen—are both significantly associated with late AMD.⁴ The distinction between conventional drusen and pseudodrusen has been made first clinically by Mimoun et al⁵ in 1990. They identified pseudodrusen as a different type of drusen based on enhanced visibility using blue light illumination and called them “les pseudo-drusen visible en lumière bleue.”⁵

Sarks et al⁶ described accumulations of membranous debris, the distinguishing component of soft drusen, on apical and basal aspects of the retinal pigment epithelium (RPE) in areas surrounding geographic atrophy. They did not make a clinical correlation, but the fundus

photographs in their paper showed dotlike structures surrounding the geographic atrophy. Rudolf et al⁷ described 3 eye bank eyes with subretinal deposition of drusenoid material that shared many histologic characteristics with soft drusen, except for location. Unlike conventional drusen on the inner portion of Bruch’s membrane external to the RPE, subretinal drusenoid deposits (SDD) were found internal to the RPE. Zweifel et al⁸ demonstrated eyes with pseudodrusen have collections of material in the subretinal space as seen using spectral-domain optical coherence tomography (SD-OCT) that have the size and shape corresponding with the pseudodrusen seen in color fundus photographs. They made the link between the material visualized in vivo and that seen in the histopathologic studies.^{6,7} Later work from the same authors showed the reflectance properties conferred by the location of the material relative to the RPE would

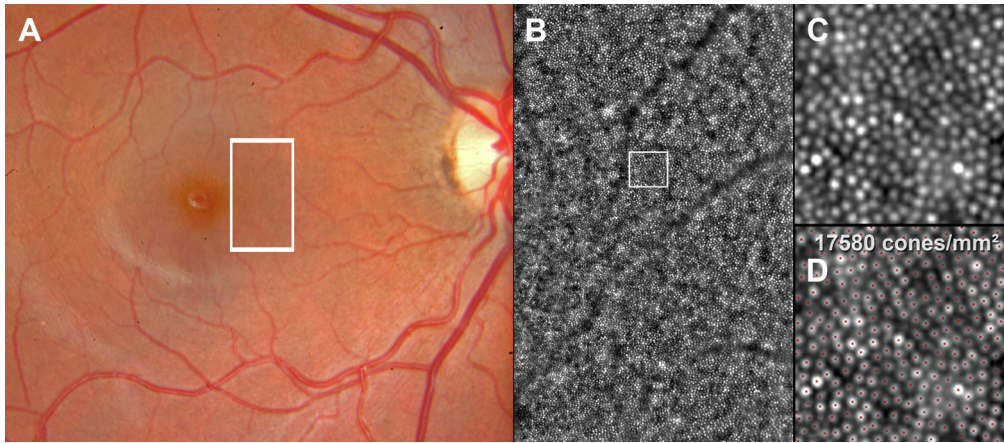


Figure 1. Method of cone packing density measurement using the software program provided by the system manufacturer (CK v0.1 and AO detect v0.1, Imaging Eyes, France) in the normal right eye of a 21-year-old female. **A**, Normal retinal appearance of the posterior pole and the adaptive optics (AO) image corresponding to the area in the white rectangle. **B**, Normal cone mosaic. The magnified AO images (**C**, **D**) correspond with the area in the white square. **D**, Red dots mark the structures that have been identified and counted automatically as cones by the software.

account for the enhanced visualization with blue light.⁹ The presence of SDD was found to be an independent risk factor for late AMD in a case control study.⁴ Limited published histologic data has shown photoreceptor degeneration internal to SDD.⁹

Photoreceptors overlying conventional drusen may show signs of degeneration in histologic study.^{10–12} Schuman et al¹³ found that there was outer nuclear layer thinning over drusen *in vivo* using SD-OCT, suggesting photoreceptor loss or at least lateral displacement. However, there is

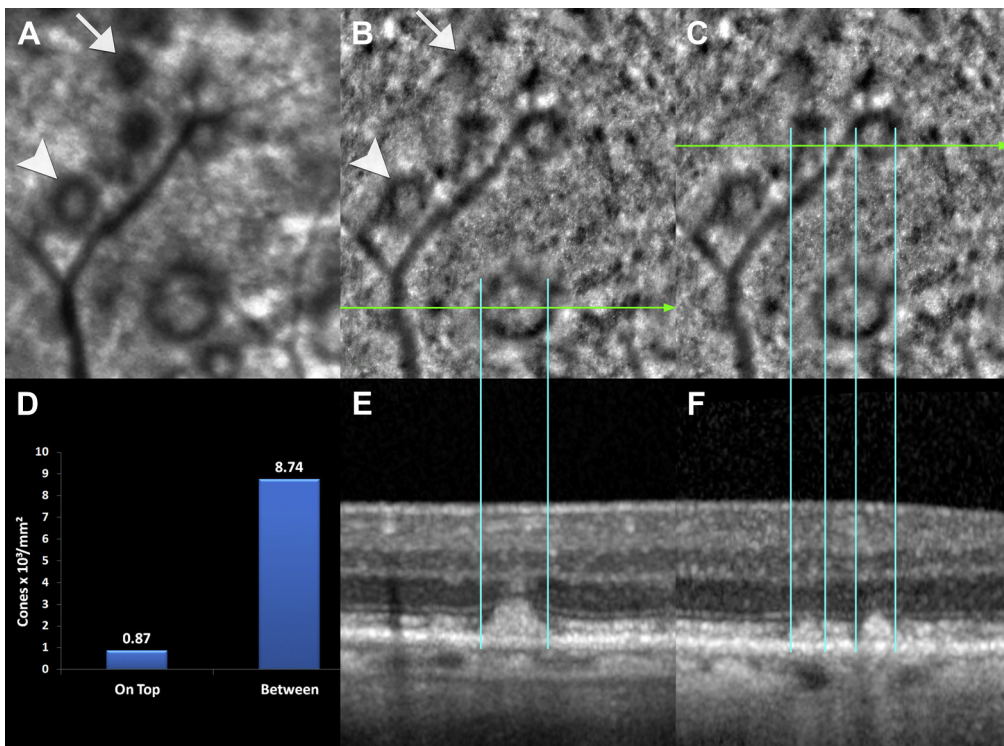


Figure 2. Multimodal imaging of the right eye of an 84-year-old woman with pseudodrusen appearance seen during the ophthalmoscopic examination. **A**, Near infrared reflectance (IR) confocal scanning laser ophthalmoscope (SLO) image and (**B** and **C**) the corresponding adaptive optics (AO) image. **D**, Cone packing density was much lower over subretinal drusenoid deposits (SDD) than in between SDD measured in that AO image. The numbers above the bars are thousands of cones per square millimeter. Multiple SDD identified by combined IR-SLO (**A**) and (**E**, **F**) on spectral-domain optical coherence tomography (SD-OCT) correspond with well-defined areas that have somewhat similar gross reflectance characteristics in the AO image as in the IR image. Some SDD seem to be completely dark (white arrow) and others have a dark annulus surrounding interiors that have similar gross intensities than those of adjacent non-SDD-bearing areas (white arrowhead). The SDD seemed to be encircled by a dark annular ring of nearly constant width that corresponded with an area where the ellipsoid zone seems to be either tilted or disrupted in corresponding SD-OCT images (blue lines).

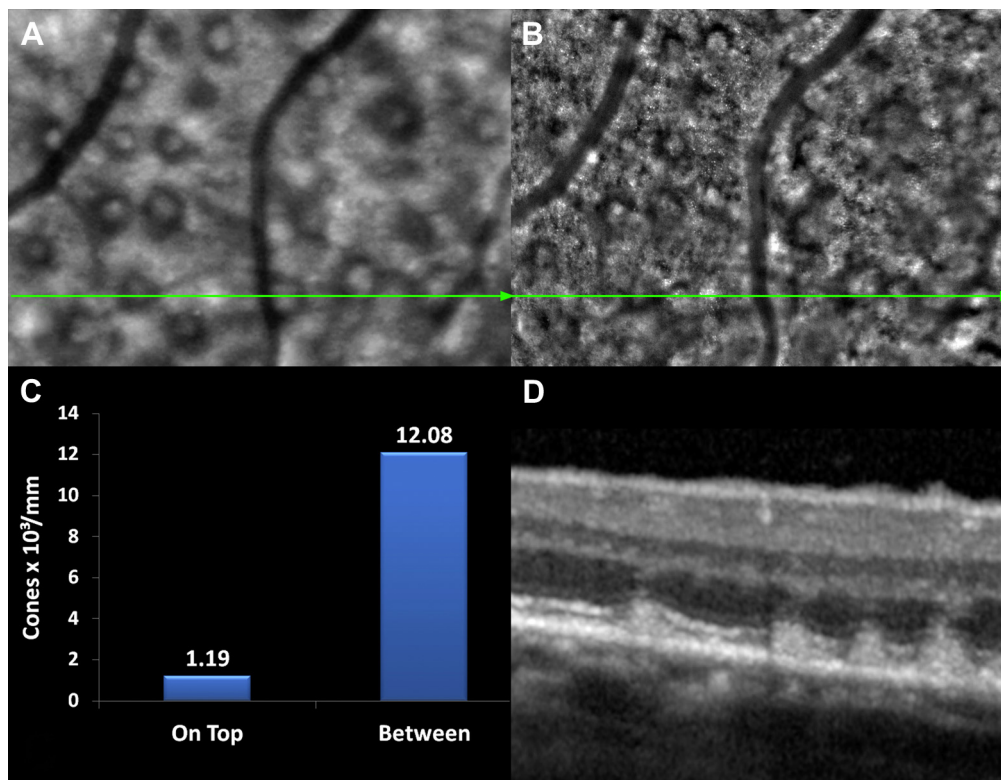


Figure 3. This 71-year-old woman had multiple pseudodrusen seen in the infrared reflectance (IR) confocal scanning laser ophthalmoscope (SLO) image (A) and corresponding adaptive optics (AO) montage (B). C, There was a marked reduction in cone packing density over subretinal drusenoid deposits (SDDs) compared with between them. D, Multiple SDD are visible in the spectral-domain optical coherence tomography (SD-OCT) image and these colocalized with the IR-SLO image showing pseudodrusen and the AO montage image (B) of the same lesions.

limited data about photoreceptor distribution over drusen *in vivo*. Conventional imaging systems cannot visualize individual photoreceptors because lateral resolution is limited by the numerical aperture of the system used and the aberrations of the human eye. Adaptive optics (AO) has been used to improve the transverse resolution of retinal imaging by measuring the optical aberrations and compensating for them in real time with active optical elements.^{14,15} Because the resolution is improved to several micrometers, cone photoreceptor packing density analysis can be performed *in vivo*. We present a preliminary analysis of cone photoreceptor density overlying pseudodrusen and soft drusen using AO imaging and these results were compared with multimodal imaging data.

Methods

This retrospective study of consecutively imaged patients with the clinical diagnosis of nonconfluent pseudodrusen and soft drusen examined patients from a private retinal referral practice between June 2012 and July 2013. The diagnosis of pseudodrusen and soft drusen in this study was based on combined color photograph, red-free photograph, near-infrared reflectance (IR) confocal scanning laser ophthalmology (SLO) and SD-OCT according to our previously established criteria.^{4,8,9} Pseudodrusen were diagnosed based on the ophthalmoscopic appearance; the material in the subretinal space as seen by OCT or AO imaging was termed SDD. The height of soft drusen was measured between the Bruch's

membrane band and the inner border of the RPE band. The height of SDD was measured between the inner portion of the RPE band to the inner border of the subretinal material. We made OCT image measurements using image planimetry software (Spectralis Viewing Module 5.4.6.0; Heidelberg Engineering, Heidelberg, Germany). The integrity of the ellipsoid zone was evaluated over SDD and conventional drusen in the SD-OCT images.¹⁶ The conventional drusen evaluated were ≥ 63 μm in diameter, thus falling in the range of medium to large drusen.¹⁷

Patients with pseudodrusen and conventional drusen were examined with a flood-illuminated retinal AO camera (rtx-1, Imagine Eyes, Orsay, France) to assess the cone photoreceptor mosaic overlying pseudodrusen and soft drusen. All patients signed an informed consent form after receiving a full explanation of the AO imaging procedure. The study had institutional review board approvals through the Western Institutional Review Board and complied with the Health Insurance Portability and Accountability Act of 1996. The study adhered to the tenets of the Declaration of Helsinki. Color photographs were obtained with a Topcon ImageNet camera (Topcon America, Paramus, NJ). The IR-SLO images and eye-tracked SD-OCT scans were obtained with the Heidelberg Spectralis (version 1.6.1, Heidelberg Engineering).

The rtx1 Adaptive Optics Retinal Camera

The rtx1 AO retinal flood-illumination camera (Imagine Eyes) is a compact device that includes a wavefront sensor (HASO 32-eye, Imagine Eyes), a correcting element (52-actuating electromagnetic deformable mirror; MIRA0 52-e, Imagine Eyes), and a low-noise, high resolution, charge-coupled device camera (Rope Scientific,

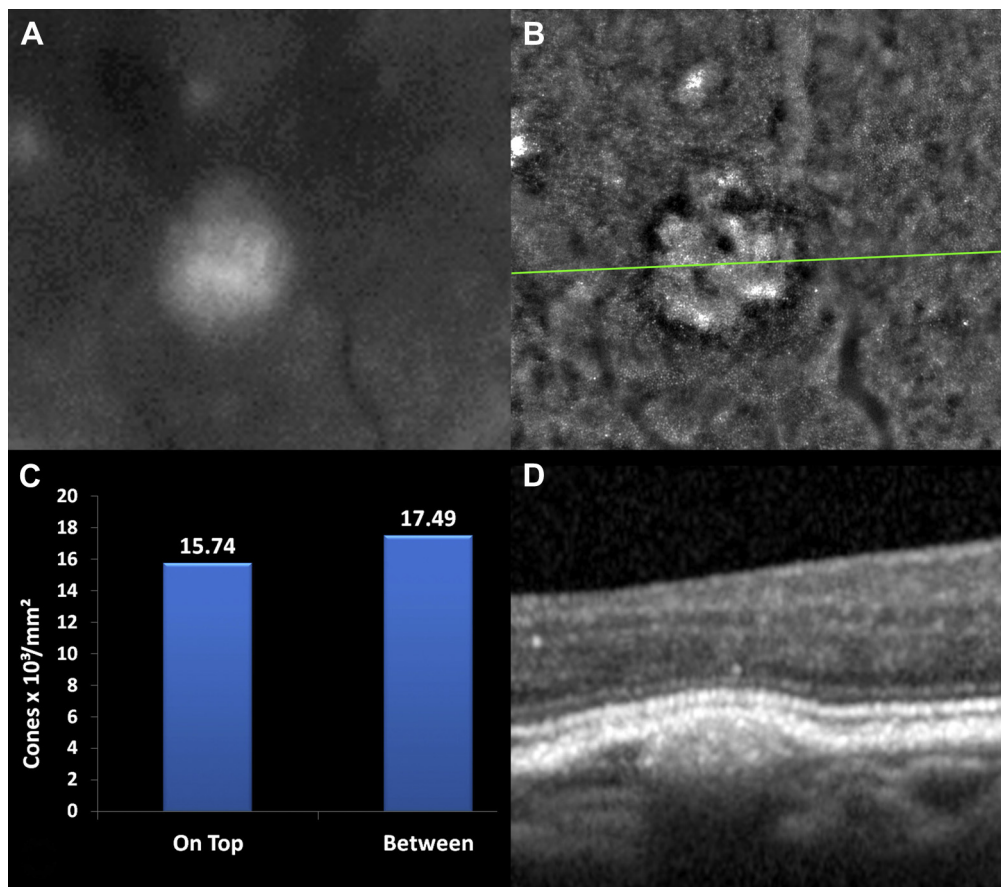


Figure 4. Multimodal imaging of the left eye of a 71-year-old woman with multiple, soft drusen seen in the ophthalmoscopic examination. **A**, Red-free photograph shows a druse that is seen in greater detail in **(B)**, the adaptive optics (AO) image. The cone density showed a modest reduction over conventional drusen as compared with between them. **D**, Spectral-domain optical coherence tomography (SD-OCT) shows the elevation of the retinal pigment epithelium (RPE) along with the retina, over a sub-RPE accumulation of material.

Tucson, AZ). The rtx1 AO system uses 2 light sources: A low-coherence superluminescent diode centered at 750 nm that is used for measuring and correcting optical aberrations and controlling the focus at the retinal layers and a light-emitting diode with a wavelength centered at 850 nm that provides uniform illumination of the retinal area imaged. The AO imaging sessions were performed with dilated pupils. Each image was obtained from an average of 40 frames of a $4^\circ \times 4^\circ$ retinal area over an acquisition time of 4 seconds. Multiple images were recorded between 1° and 8° of retinal eccentricity from the foveal center in the areas of SDD and soft drusen identified using combined IR and eye-tracked SD-OCT images as a guide. We carefully focused the AO camera through the depth of the retina to detect reflectivity consistent with cone inner segments overlying both SDD and soft drusen.

Postprocessing Methods for Adaptive Optics Imaging

Each series of 40 images acquired by the AO camera was processed using software programs provided by the system manufacturer (CK v0.1 and AOdetect v0.1, Imagine Eyes). These images were registered and averaged to produce a final image with improved signal-to-noise ratio. The raw images that showed artifacts owing to eye blinking and saccades were automatically eliminated before averaging. For display and printing purposes, the histogram of the resulting averaged image was stretched over a 16-bit range of gray levels. The positions of photoreceptor inner

segments were computed by automatically detecting the central coordinates of small circular spots whose brightness differed from the surrounding background level. The spatial distribution of these point coordinates was finally analyzed in terms of local cell numerical density (cells per square millimeter of retinal surface).

For each patient, cone packing density analysis was performed on AO images within $50 \times 50\text{-}\mu\text{m}$ windows in 5 regions of interest overlying and in 5 located between SDD and soft drusen. Each measurement of cone density on top of SDD or soft drusen was paired with a measurement in between drusen at approximately the same degree of retinal eccentricity from the foveal center in the same quadrant. The regions of interest in eyes with SDD and eyes with conventional drusen were not necessarily at the same retinal eccentricity. The cone packing density measurements were performed using software programs provided by the system manufacturer (CK v0.1 and AOdetect v0.1, Imagine Eyes), as described (Fig 1).

Correlations between the Different Modalities of Imaging

For each eye, Photoshop (Photoshop CS6, Adobe System Inc, San Jose, CA) was used to superimpose the color photograph, the IR-SLO image, and each AO image manually, using the retinal vessels as landmarks. The correlation feature of the Heidelberg Spectralis was used to establish the correspondence between the



Figure 5. Schematic representing the reflectivity profile of subretinal drusenoid deposits (SDD) in both the infrared reflectance (IR) confocal scanning laser ophthalmoscope (SLO) and adaptive optics (AO) images. The smallest SDD seems to be completely dark and the others have a dark annulus surrounding interiors that had intensities grossly similar to those of adjacent non-SDD-bearing areas. The dark annulus is approximately the same width in all cases, independent of the diameter of the SDD itself.

IR-SLO image and the SD-OCT image. Manual corrections to correlations were made using Photoshop if the retinal vessels in the SD-OCT scans did not accurately match with the IR-SLO images of the same retinal vessels. Then, correlations were made between the IR-SLO and the matched color photographs, IR-SLO, and AO images.

Statistical Analysis

Correlations were made between mean cone packing density over drusen and disruption of the ellipsoid zone over drusen and the diameter and the height of the drusen in SD-OCT images, using a generalized estimating equation analysis. The statistical analyses were performed with SPSS software version 20.0 (SPSS, Inc, Chicago, IL). $P < 0.05$ was considered significant.

Results

The mean \pm standard deviation age of 11 patients with SDD was 75.7 ± 7.42 years; 2 patients were males. The mean age of 6 patients (11 eyes) with conventional (soft) drusen was 71.7 ± 7.27 years; 2 patients were males. The difference in ages was not significant ($P = 0.216$). Nonexudative AMD was present in 10 eyes with SDD and 10 eyes with soft drusen. Subfoveal choroidal neovascularization was present in 1 eye with conventional drusen and 1 eye with SDD. One patient with SDD had a pigmented foveal scar owing to subretinal neovascularization secondary to macular telangiectasia type 2. The areas imaged were never directly involved with exudation. The SDD identified by combined IR-SLO and SD-OCT corresponded with well-defined areas darker than the surrounding uninvolved areas in the AO images (Figs 2 and 3). The size, shape, and reflectivity of the SDD varied in the AO images and correlated with their size, shape, and reflectivity in the corresponding IR-SLO images.

The conventional drusen identified by combined color photographs, IR-SLO, and SD-OCT corresponded with areas of subtle alterations in grayscale intensity in the AO images (Fig 4). Lesion size and shape varied and showed a correspondence between the IR-SLO images and color photographs (Fig 4). The mean greatest linear diameter measured for drusen evaluated with AO

imaging was 234 ± 189.8 μm , which was larger than the SDD (119 ± 18.4 μm ; $P = 0.086$). The mean height of the conventional drusen was 60 ± 20.3 μm , compared with the height of the SDD (74 ± 13.4 μm ; $P = 0.091$). Fifty-five SDD and 55 conventional drusen were analyzed.

The mean cone packing density was 8964 ± 2793 cones/ mm^2 between SDD as compared with 863 ± 388 cones/ mm^2 over SDD, a 90.4% reduction in cone density. The mean cone packing density was 9838 ± 3723 cones/ mm^2 over conventional drusen and 12592 ± 3323 cones/ mm^2 between conventional drusen, a 21.9% reduction. The proportions of cone density reduction over SDD compared with conventional drusen was highly significant ($P < 0.001$). The ellipsoid zone was intact over all of the conventional drusen. The observed densities are within the range of densities determined histologically from grossly normal older donor retinas from similar eccentricities.¹⁸

Thirty-one SDD seemed to be completely dark in AO images. Twenty-four others had a dark annulus surrounding a central region with intensities grossly similar to those of adjacent non-SDD-bearing areas (Fig 2). The dark annulus was approximately the same width in all cases, independent of the diameter of the SDD itself (Figs 2, 3, and 5) and corresponded with loss or distortion of the ellipsoid zone in corresponding SD-OCT images (Fig 2).

Discussion

In this study of both SDD and conventional drusen, imaging data from color photographs, IR-SLO, SD-OCT, and AO images provided converging evidence about the site of both lesions. Subretinal drusenoid deposits localized specifically to the subretinal space and conventional drusen to the sub-RPE space. Cone density was dramatically reduced over SDD in the AO images. By comparison, cone density was relatively preserved over conventional drusen in the AO images. The lack of visualization of cones over SDD in the AO images can be owing to several causes impacting reflectivity including a change in their orientation, absence, or shortening of the inner or outer segments or both, or loss

of cones in totality. There was no difference in the heights of the respective lesions, implying a true structural difference in photoreceptor configuration. With conventional drusen the RPE is displaced by the sub-RPE material, and the retina seems to conform to variations induced by the underlying contour of the RPE monolayer. With SDD, the extracellular material physically juts into the subretinal space, in close proximity to photoreceptors, and as a consequence alters the outer retinal structure as visualized by both AO imaging and SD-OCT. To the best of our awareness, there has not been a previously published study using AO to evaluate cone density in eyes with AMD.

These new findings from AO imaging integrated into a multimodal approach are consistent with previously published results^{4,8,9} that pseudodrusen appearance is the result of subretinal deposition of material. These findings are not consistent with alternate hypotheses, such as the appearance is owing to alterations of the RPE¹⁹ or patterns within the choroid.²⁰ These new AO imaging observations suggest that the different imaging aspects of SDD correspond to different stages of a progressive disease, as has been previously suggested in the literature^{8,21,22} and that the material accumulates in the same tissue compartment as the photoreceptors.

The cone mosaic was previously evaluated over 1 conventional druse in a 45-year-old asymptomatic woman²³ and over large colloid drusen in a 29-year-old woman.²⁴ The results of the case reports were consistent with what was found in the present series. Reduction in cone packing density over conventional drusen was modest. In our study, the packing density over SDD was distinctly decreased, and the magnitude of this reduction was apparent when compared with that over conventional drusen. To the best of our knowledge, there has been no previous report evaluating the differential loss of photoreceptors overlying SDD versus conventional drusen, by histopathology or in vivo. With AMD progression there is the potential for an increasing confluence of SDD and of conventional drusen. The outer retinal abnormalities seen over isolated SDD would likely be present in more confluent phenotypes. Thus, increasing areas of SDD would be associated with more profound areas of photoreceptor absence detectable by high-resolution imaging. It is also likely that there would be alterations in the cone packing density over confluent areas of conventional drusen, but given the diminution of cones was less severe over isolated conventional drusen, the decrease in cone packing density is likely to be not as bad as over confluent SDD. In support of this hypothesis is the long-term observation that visual acuity in eyes with conventional drusen under the fovea usually is good.²⁵ Confluent areas of SDD are not typically observed in the fovea.

The SDD phenotype seems to be more threatening to vision and quality of life than the conventional drusen phenotype. These new results from AO retinal imaging are consistent with the handicapping visual complaints of patients with pseudodrusen despite a relatively preserved fundus examination and the absence of late AMD according to the current terminology. Spaide²² recently described outer retinal atrophy as a common finding in eyes having

pseudodrusen using OCT and proposed to add this entity as a new type of late AMD that can overlap with geographic atrophy and choroidal neovascularization.²²

The limitations of this preliminary study are that it is an observational case series with a small number of patients. The comparison of paired within-eye observations was a strength because it obviates variability introduced by rapidly changing cone densities with increasing eccentricity and differences between patients.^{10,26} Image acquisition with AO systems and the subsequent image processing is extremely time consuming, which currently limits more widespread application. Future studies are required to evaluate eyes with different stages of SDD in AMD over time and the dynamics of photoreceptor distribution overlying different types of drusen. If cone photoreceptor function is reduced in proportion with the observed cone packing density, then eyes with pseudodrusen appearance, particularly with confluent SDD, are likely to have decreased photopic visual function. The rods were not visualized in this study, but given that rods may be affected before cones in both aging and AMD,²⁷ the results of this study do not imply that visual function mediated by rods will be normal. As a consequence, we have started a prospective study examining functional tests, including microperimetry, in relation to lesion type. In addition, we have begun to examine the histologic characteristics of photoreceptors over collections of SDD in autopsy eyes.

References

1. Eye Diseases Prevalence Research Group. Causes and prevalence of visual impairment among adults in the United States. *Arch Ophthalmol* 2004;122:477–85.
2. Klein R, Klein BE, Jensen SC, Meuer SM. The five-year incidence and progression of age-related maculopathy: the Beaver Dam Eye Study. *Ophthalmology* 1997;104:7–21.
3. Mitchell P, Smith W, Attebo K, Wang JJ. Prevalence of age-related maculopathy in Australia. The Blue Mountains Eye Study. *Ophthalmology* 1995;102:1450–60.
4. Zweifel SA, Imamura Y, Spaide TC, et al. Prevalence and significance of subretinal drusenoid deposits (reticular pseudodrusen) in age-related macular degeneration. *Ophthalmology* 2010;117:1775–81.
5. Mimoun G, Soubrane G, Coscas G. Macular drusen [in French]. *J Fr Ophtalmol* 1990;13:511–30.
6. Sarks JP, Sarks SH, Killingsworth MC. Evolution of geographic atrophy of the retinal pigment epithelium. *Eye (Lond)* 1988;2:552–77.
7. Rudolf M, Malek G, Messinger JD, et al. Sub-retinal drusenoid deposits in human retina: organization and composition. *Exp Eye Res* 2008;87:402–8.
8. Zweifel SA, Spaide RF, Curcio CA, et al. Reticular pseudodrusen are subretinal drusenoid deposits. *Ophthalmology* 2010;117:303–12.
9. Spaide RF, Curcio CA. Drusen characterization with multimodal imaging. *Retina* 2010;30:1441–54.
10. Curcio CA, Medeiros NE, Millican CL. Photoreceptor loss in age-related macular degeneration. *Invest Ophthalmol Vis Sci* 1996;37:1236–49.
11. Johnson PT, Brown MN, Pulliam BC, et al. Synaptic pathology, altered gene expression, and degeneration in

- photoreceptors impacted by drusen. *Invest Ophthalmol Vis Sci* 2005;46:4788–95.
12. Johnson PT, Lewis GP, Talaga KC, et al. Drusen-associated degeneration in the retina. *Invest Ophthalmol Vis Sci* 2003;44:4481–8.
 13. Schuman SG, Koreishi AF, Farsiu S, et al. Photoreceptor layer thinning over drusen in eyes with age-related macular degeneration imaged in vivo with spectral-domain optical coherence tomography. *Ophthalmology* 2009;116:488–96.
 14. Hofer H, Chen L, Yoon GY, et al. Improvement in retinal image quality with dynamic correction of the eye's aberrations. *Opt Express* [serial online] 2001;8:631–43. Available at: <http://www.opticsinfobase.org/oe/abstract.cfm?uri=oe-8-11-631>. Accessed September 14, 2013.
 15. Liang J, Williams DR, Miller DT. Supernormal vision and high-resolution retinal imaging through adaptive optics. *J Opt Soc Am A Opt Image Sci Vis* 1997;14:2884–92.
 16. Spaide RF. Questioning optical coherence tomography. *Ophthalmology* 2012;119:2203–4.
 17. Ferris FL III, Wilkinson CP, Bird A, et al. Beckman Initiative for Macular Research Classification Committee. Clinical classification of age-related macular degeneration. *Ophthalmology* 2013;120:844–51.
 18. Curcio CA, Millican CL, Allen KA, Kalina RE. Aging of the human photoreceptor mosaic: evidence for selective vulnerability of rods in central retina. *Invest Ophthalmol Vis Sci* 1993;34:3278–96.
 19. Smith RT, Chan JK, Busuoic M, et al. Autofluorescence characteristics of early, atrophic, and high-risk fellow eyes in age-related macular degeneration. *Invest Ophthalmol Vis Sci* 2006;47:5495–504.
 20. Sohrab MA, Smith RT, Salehi-Had H, et al. Image registration and multimodal imaging of reticular pseudodrusen. *Invest Ophthalmol Vis Sci* 2011;52:5743–8.
 21. Querques G, Canoui-Poitine F, Coscas F, et al. Analysis of progression of reticular pseudodrusen by spectral domain-optical coherence tomography. *Invest Ophthalmol Vis Sci* 2012;53:1264–70.
 22. Spaide RF. Outer retinal atrophy after regression of subretinal drusenoid deposits as a newly recognized form of late age-related macular degeneration. *Retina* 2013;33:1800–8.
 23. Godara P, Siebe C, Rha J, et al. Assessing the photoreceptor mosaic over drusen using adaptive optics and SD-OCT. *Ophthalmic Surg Lasers Imaging* 2010;41(suppl):S104–8.
 24. Querques G, Massamba N, Guigui B, et al. In vivo evaluation of photoreceptor mosaic in early onset large colloid drusen using adaptive optics [letter][report online]. *Acta Ophthalmol* 2012;90:e327–8. Available at: <http://onlinelibrary.wiley.com/doi/10.1111/j.1755-3768.2011.02228.x/pdf>. Accessed September 14, 2013.
 25. Leibowitz HM, Krueger DE, Maunder LR, et al. The Framingham Eye Study monograph: An ophthalmological and epidemiological study of cataract, glaucoma, diabetic retinopathy, macular degeneration, and visual acuity in a general population of 2631 adults, 1973-1975. *Surv Ophthalmol* 1980;24(suppl):335–610.
 26. Curcio CA, Sloan KR, Kalina RE, Hendrickson AE. Human photoreceptor topography. *J Comp Neurol* 1990;292:497–523.
 27. Jackson GR, Owsley C, Curcio CA. Photoreceptor degeneration and dysfunction in aging and age-related maculopathy. *Ageing Res Rev* 2002;1:381–96.

Footnotes and Financial Disclosures

Originally received: March 23, 2013.

Final revision: August 19, 2013.

Accepted: September 18, 2013.

Available online: ■■■■.

Manuscript no. 2013-479.

¹ Vitreous Retina Macula Consultants of New York, New York, New York.

² LuEsther T. Mertz Retinal Research Center, Manhattan Eye, Ear, and Throat Hospital, New York, New York.

³ Department of Ophthalmology, University of Alabama at Birmingham, Birmingham, Alabama.

Financial Disclosures:

The authors have made the following disclosures: Richard F. Spaide: Consultant, Royalties—Topcon; Consultant—Thrombogenics; Consultant—Bausch and Lomb.

Christine A. Curcio:

Research Support—Genentech; Consultant—Hoffman-LaRoche; Research Support—Rinat Neuroscience/ Pfizer.

Supported by the LuEsther T. Mertz Retinal Research Foundation. C.A.C. is supported by NEI EY06109 with institutional support from the EyeSight Foundation of Alabama and Research to Prevent Blindness Inc.

Correspondence:

Richard F. Spaide, MD, Vitreous Retina Macula Consultants of New York, 460 Park Avenue, Fifth Floor, New York, NY 10022. E-mail: rick.spaide@gmail.com.